Real-time vibration measurement using a feedback type of laser diode interferometer with an optical fiber

Takamasa Suzuki,* MEMBER SPIE
Takao Okada
Osami Sasaki
Takeo Maruyama
Niigata University
Faculty of Engineering
8050 Ikarashi 2
Niigata 950-21, Japan
E-mail: takamasa@eng.niigata-u.ac.jp

Abstract. A laser diode interferometer that uses an optical fiber is proposed. The laser diode simultaneously functions as a light source, a phase modulator, and a phase compensator. Detection of the vibration and reduction of external disturbance are carried out using a feedback control for the injection current of the laser diode. Thus it can measure vibration accurately in real time with a simple signal processing circuit. The optical fiber not only functions as a flexible probe, enabling us to measure the vibration of an object that cannot be moved onto the optical bench, it also acts as a reference mirror, thereby simplifying the unit construction. The principle of the feedback control in laser diode interferometer is also described in detail. [S0091-3286(97)01109-4]

Subject terms: interferometer; laser diode; optical fiber; feedback control; vibration measurement.

Paper 18126 received Dec. 10, 1996; revised manuscript received Apr. 1, 1997; accepted for publication Apr. 1, 1997. This paper is a revision of a paper presented at the SPIE conference on Laser Interferometry VII, August 1996, Denver, CO. The paper presented there appears (unrefereed) in the Proceedings of SPIE Vol. 2860.

1 Introduction

Although optical interferometry is useful for the precise measurement of vibration and surface profile, because no physical contact is necessary, conventional types of interferometers do have certain disadvantages: (1) measuring displacements that exceed a half wavelength requires phase unwrapping to obtain accurate displacement; (2) the interferometer itself is vulnerable to external disturbance, therefore measurement must be carried out on an optical bench; (3) a complicated signal processing system is required to measure vibration in real time; and (4) it is difficult to measure the vibration of an object that cannot be moved onto the optical bench. To overcome these problems, we devised a "feedback" type of laser diode (LD) interferometer equipped with an optical fiber. The LD is used as a light source, a phase modulator,[1] and a phase compensator simultaneously in this interferometer.

The feedback is very useful to eliminate the external disturbance in real time, and was used in the previous studies.[2-5] Besides, the feedback can be used for the measurement of vibration[2] or surface profile. The measurement of surface profile can be realized accurately by using the phase-locked technique[6-8] for a fixed object. On the other hand, for a vibrating object, changes in the feedback signal represent the vibration of the object. However, since the observed signal does not tell us the amplitude of the vibration exactly, the observed amplitude must be calibrated with an amplitude observed by other methods. Here we present a theoretical analysis of the relationship between the observed signal and the actual amplitude. The accurate vibration measurement is then carried out in real time by observing the feedback signal.

In addition, the need for phase unwrapping is eliminated in this type of interferometer because the phase change is minimized by the feedback control. External disturbance is also eliminated in this interferometer, by the same mechanism.[2-5] This compensation is realized by adjusting the amount of feedback in the LD injection current. Consequently, while the measurement range is expanded, and distortion is reduced to insignificant levels.

Other advantages of this system lie in the extensive use of optical fiber. First, since a reflected light from the exit face of the optical fiber is used as a reference beam in our system, the optical system itself becomes a sort of simple Fizeau type of interferometer[9] and is therefore itself insensitive to external disturbance. Second, the system enables the placement of the probe at virtually any location.

In Sec. 2, this paper first describes the measurement principle and then discusses a theoretical treatment of the feedback control system in detail. The experimental results are shown in Sec. 3, where we discuss the difference of the measurable range depending on the control system.

2 Principle

2.1 *Configuration of the Experimental Setup*

The configuration of our interferometer is shown in Fig. 1. The light from the LD is collimated with lens L1 and passed through an optical isolator, a beamsplitter (BS), and an optical fiber. Part of the beam passing through the fiber

*Current affiliation: University of Arizona, Optical Sciences Center, Tucson, AZ 85721.

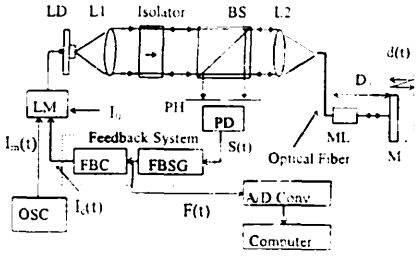

Fig. 1 Experimental setup of the feedback-type LD interferometer: LD, laser diode; LM, laser diode modulator; ML, microlens; FBC, feedback controller; FBSG, feedback signal generator; PD, photodetector; and PH, pin hole.

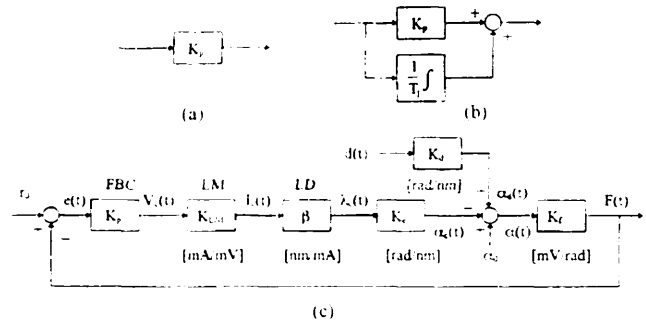

Fig. 2 Block diagram of the control system. One of two kinds of FBCs, that is (a) a proportional controller or (b) a proportional-integral controller, is used in the experiments, and (c) the proportional control system: K_p, proportional gain; K_{LM}, gain of the LD modulator; β, modulation efficiency of the LD; K_c, gain depending on the optical path difference; K_d, transfer function from the displacement of the object to phase change; and K_f, amplitude of the feedback signal.

is reflected back from the exit face and is used as a reference beam. The output beam from the fiber is collimated with a microlens (ML) and irradiates the object mirror (M). The reference and object beams whose optical pass difference is $2D_0$ return to the same pass. They are then detected by a photodetector (PD) as an interference signal $S(t)$. Therefore, a Fizeau-type interferometer is constructed in our optical system. The signal $S(t)$ is fed in sequence to the LD, first, through a feedback system and, then, an LD modulator (LM) to compensate for the phase change caused by the vibration $d(t)$ of the object. The injection current of the LD consists of dc bias current I_0, modulation current $I_m(t)$, and control current $I_c(t)$ generated from $S(t)$. The central wavelength λ_0 is determined by I_0. The modulation current is given by

$$I_m(t)=a\cos\omega_c t, \tag{1}$$

which alters the wavelength of LD by $\beta I_m(t)$ and provides for the direct modulation of the interference signal, where β is a modulation efficiency of the LD. Then, $S(t)$ is given by

$$S(t)=S_1+S_0\cos[z\cos\omega_c t+\alpha_0+\alpha_d(t)], \tag{2}$$

where S_1 and S_0 are the dc component and the amplitude of the ac component, respectively; $z=4\pi a\beta D_0/\lambda_0^2$ is a modulation coefficient;

$$\alpha_0=\frac{4\pi}{\lambda_0}D_0 \tag{3}$$

is an initial constant phase determined by the optical path difference $2D_0$; and

$$\alpha_d(t)=\frac{4\pi}{\lambda_0}d(t) \tag{4}$$

is a phase change introduced by the vibration $d(t)$. To realize a feedback control for the compensation of phase change, the feedback signal that contains $\alpha_d(t)$ is required.

The feedback signal is created in the feedback-signal generator (FBSG) shown in Fig. 1. It multiplies modulation signal $I_m(t)$ and interference signal $S(t)$, and passes the product through a low-pass filter (LPF), the cutoff frequency of which is lower than one tenth of the modulation frequency. Then the carrier component is removed sufficiently and the feedback signal,

$$F(t)=K_f\sin[\alpha_0(t)+\alpha_d(t)]\approx K_f\alpha(t), \tag{5}$$

is obtained,[3] where K_f is an amplitude of the feedback signal and $\alpha(t)=\alpha_0+\alpha_d(t)$. Since the gradient of $\sin\alpha(t)$ is unity near $\alpha(t)=2n\pi$, the feedback signal is approximated to $K_f\alpha(t)$ around the point of origin. Feedback signal $F(t)$ is then fed into the feedback controller (FBC) and control current $I_c(t)$ is injected into the LD through the LM. Then the phase of the interference signal is compensated. We explain the principle of the phase compensation in the following sections.

2.2 *Block Diagram of the Control System*

To simplify the explanation, we consider a vibration whose frequency is much lower than the cutoff frequency of the LPF. Then, the influence of the LPF is negligible. A block diagram of the control system is shown in Fig. 2. In our experiments, a proportional (P) controller or a proportional-integral (PI) controller was used as the FBC. An amplifier whose gain is K_p is used as the P controller, as shown in Fig. 2(a). The PI controller is constructed with the amplifier used in the P controller, an integrator whose integral time is T_I, and an adder, as shown in Fig. 2(b). Figure 2(c) shows the scheme of the P control system. The units are represented under each transfer function. The FBC converts the error signal $e(t)$ to the control voltage $V_c(t)$, and the LM converts it to the control current $I_c(t)$. Their gains are K_p and K_{LM}, respectively. The modulation efficiency β of the LD represents a rate of the wavelength change corresponding to the injection current. The K_c is a transfer function from $\lambda_c(t)$ to $\alpha_c(t)$ and its gain is discussed in the following section. The $K_d=4\pi/\lambda_0$ is a transfer function from $d(t)$ to $\alpha_d(t)$, which is given by Eq. (4). Gain K_f, the amplitude of the feedback signal, occurs at the interferometer and the FBSG and is shown in Eq. (5).

2.3 *P Control System*

When only an amplifier whose gain is K_p is used as the FBC, the control current $I_c(t)$ changes the wavelength of the LD by $\lambda_c(t)=\beta I_c(t)$. Then the phase of the interference signal is given by

$$\alpha(t)=\frac{4\pi[D_0+d(t)]}{\lambda_0+\lambda_c(t)}\approx\alpha_0+[\alpha_d(t)-\alpha_c(t)], \tag{6}$$

where

$$\alpha_c(t)=\frac{4\pi D_0}{\lambda_0^2}\lambda_c(t) \tag{7}$$

is a compensating phase introduced by the feedback control. Therefore, the gain K_c is given by $4\pi D_0/\lambda_0^2$ as a coefficient of $\lambda_c(t)$ from Eq. (7). Since the K_c is determined by the ratio between D_0 and λ_0^2, it becomes quite large compared with the other gains and contributes to the phase compensation strongly. Thus, it enables us to reduce the control current $I_c(t)$ for phase compensation. Then, the intensity modulation in the LD induced by the injection current is negligible. The phase change is then compensated by $\alpha_c(t)$.

Consequently, under P control, the observed signal or the feedback signal $F(t)$ is given by

$$F(t)=\frac{G_0}{1+G_0}r_0+\frac{K_dK_f}{1+G_0}d(t), \tag{8}$$

where

$$G_0=K_pK_{LM}\beta K_cK_f \tag{9}$$

is a loop gain. Since the reference signal r_0 is set to zero in our system, the center of vibration of the phase is moved to the point of origin by this feedback control. Then, from Eq. (8), the vibration $d(t)$ is represented by

$$d(t)=\frac{1+G_0}{K_dK_f}F(t). \tag{10}$$

If the loop gain is much greater than unity, Eq. (10) can be rewritten simply by

$$d(t)\approx\frac{K_{LM}\beta K_c}{K_d}K_pF(t). \tag{11}$$

Since the coefficient K_f is not contained in this formula, the fluctuation of the amplitude of the interference signal does not contribute very much to the measurement accuracy.

2.4 *PI Control*

When an amplifier and an integrator are used as the FBC, the control voltage $V_c(t)$ is given by

$$\begin{aligned}V_c(t)&=K_pe(t)+\frac{1}{T_I}\int e(t)\,dt\\&=-K_pK_f\alpha_d(t)-\left[K_pK_f\alpha_0+\frac{K_f}{T_I}\int\alpha_0\,dt\right]\\&\quad-\frac{K_f}{T_I}\int\alpha_d(t)\,dt,\end{aligned} \tag{12}$$

because the error signal $e(t)$ is $-F(t)=-K_f[\alpha_0+\alpha_d(t)]$, when the feedback loop is opened, where T_I is an integral time. If the vibration of the object is periodic, such as a sinusoidal signal, the integration of the last term in Eq. (12) becomes zero. The first term and the second term change the wavelength of the LD by $\lambda_c(t)=\beta I_c(t)$ and $\lambda_b=\beta I_b$, respectively, where I_b is a dc control current generated by the integral control. The wavelength changes $\lambda_c(t)$ and λ_b compensate for the phase change introduced by the vibration of the object and the initial phase, respectively. This is explained by the following formula, which is the same as Eq. (6):

$$\alpha(t)=\frac{4\pi[D_0+d(t)]}{\lambda_0+\lambda_b+\lambda_c(t)}\approx(\alpha_0-\alpha_b)+[\alpha_d(t)-\alpha_c(t)], \tag{13}$$

where

$$\alpha_b(t)\approx\frac{4\pi D_0}{\lambda_0^2}\lambda_b \tag{14}$$

is a compensating phase generated by the integral control, and it compensates the initial phase α_0 to be zero completely. Therefore, the second term in Eq. (12) becomes zero. The phases α_0, α_b, and $\alpha_c(t)$ are represented by Eqs. (3), (4), and (7), respectively. In this case, the vibration $d(t)$ is also given by Eq. (10).

2.5 *Operating Point on the Feedback Signal*

Here it is necessary to explain the illustration of the center of vibration of the phase or the operating point on the feedback signal shown in Fig. 3. When the feedback loop is opened, the operating point is as illustrated in Fig. 3(a). While $d(t)$ is small, the observed signal or the feedback signal $F(t)$ is proportional to $d(t)$, because $\sin\alpha(t)$ is almost linear near the point of origin. But when the phase of the operating point extends beyond the region of $\pm\pi/2$ as a result of vibration of the object, the observed signal is distorted, as shown in Fig. 3(a).

However, when the feedback loop is closed and the P control works, the operating point is as illustrated in Fig. 3(b). The operating point is caused to return to its original position as a result of phase compensation. The nonlinearity in the feedback signal $\sin\alpha(t)$ is also compensated by the feedback control even if the operating point is not around the point of origin, so long as the compensated phase of the operating point is not beyond the region mentioned previously. Thus, the observed signal is not actually distorted by the phase change caused by the vibration of the object. If the phase of the operating point, however, moves out of that region, by force of extremely large vibrations,

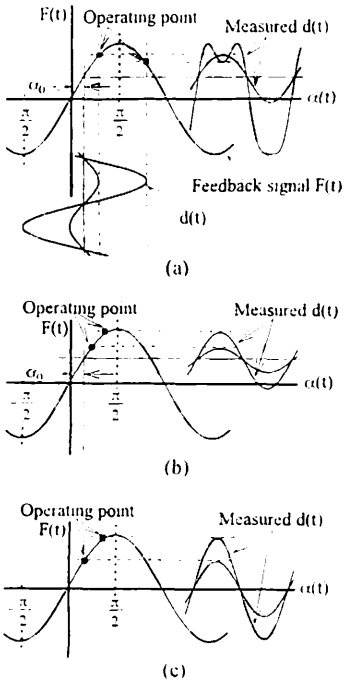

Fig. 3 Schematic explanations of the operating point on the feedback signal: (a) feedback off, (b) P control, and (c) PI control.

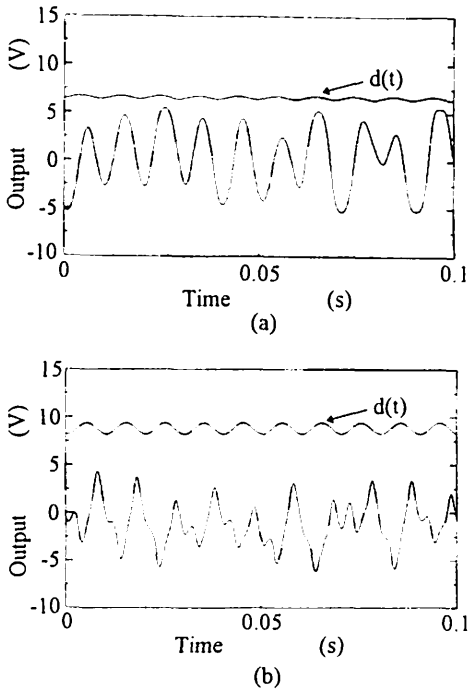

Fig. 4 Feedback signals observed when the proportional gain was zero. Upper traces indicated by $d(t)$ are sinusoidal driving signals applied to the PZT; lower traces are the feedback signals obtained when the amplitudes of $d(t)$ were (a) 50 nm and (b) 240 nm.

the feedback loop destabilizes, thus precipitating oscillation. Dynamic range and feedback loop gain increase consequently, but unfortunately the stability of the feedback loop is deteriorated in the process. In the case of Figs. 3(a) and 3(b), the observed signals contain offset signals, because of the existence of initial phase α_0. It restricts the measurable range in the P control.

To avoid this restriction, the PI control is useful. The operating point in the PI control is as illustrated in Fig. 3(c). The initial phase α_0 becomes zero, and the offset signal is automatically removed by the integral control. Then a maximum dynamic range can be obtained in the vibration measurement.

3 Experiments

The experimental setup is shown in Fig. 1. The central wavelength λ_0, maximum output power, and modulation efficiency β are 670 nm, 10 mW, and 4×10^{-3} nm/mA, respectively. The object mirror is mounted on a piezoelectric transducer (PZT). The vibration amplitude of the PZT, which depends on the applied voltage, was calibrated with the other interferometer. The length and diameter of the optical fiber are 600 mm and 80 μm, respectively. The optical path difference $2D_0$ is 200 mm. The diameter of the irradiated area on the object mirror was 3 mm. The modulation frequency of the LD was 10 kHz in all experiments. In this instance, we used a second-order LPF whose cutoff frequency was 400 Hz. Thus, the frequency response of this system is less than 400 Hz. But the response can be improved by increasing the modulation frequency. The modulation coefficient z of the sinusoidal phase modulation was 2.53. The gain K_{LM} is 1.3×10^{-2} mA/mV. The transfer function K_c, given by Eq. (7), becomes 3.16×10^3 rad/nm. The amplitude K_f of the feedback signal was set to 4.52×10^3 mV/rad.

First, we measured sinusoidal vibrations of the mirror by changing the proportional (P) gain K_p in connection with the explanations in Fig. 3. The frequency of all the vibrations were 100 Hz, which is smaller than the cutoff frequency of the LPF. All results described in this section were obtained in real time. The measurement results obtained when the feedback loop was opened or the P gain $K_p=0$ are shown in Fig. 4. The upper traces indicated by $d(t)$ are driving signals applied to the PZT. These correspond to the schematic explanation shown in Fig. 3(a). The vibration amplitudes in Figs. 4(a) and 4(b) were 50 and 240 nm, respectively. Since the phase change caused by the vibration is small enough in Fig. 4(a), the operating point does not exceed the region of $\pm\pi/2$. Although external disturbances were superimposed, the observed signal followed the mirror vibration. The maximum amplitude and frequency of the mechanical disturbance were $\sim$100 nm and less than 100 Hz in this experiment. On the other hand, when the displacement of the mirror became larger than a half wavelength of the LD, the observed signal deviated markedly from the mirror vibration, as shown in Fig. 4(b).

When the P control was worked with K_p at 0.28, where loop gain G_0 was 20 in this case, the measurable amplitude of the vibration was dramatically increased to 1440 nm, and the influence of the external disturbance is also suppressed very well, as shown in Fig. 5(a), because the phase change of the operating point was suppressed by the feedback control. When the amplitude of the vibration became 1640 nm.

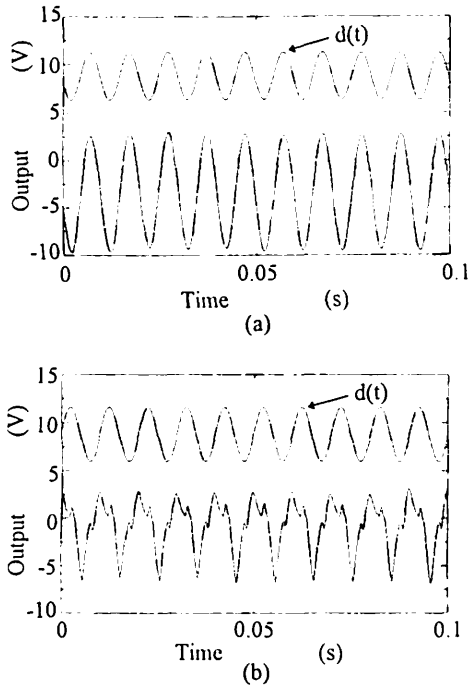

Fig. 5 Feedback signals observed when P control was used. Lower traces are the feedback signals obtained when the amplitudes of $d(t)$ were (a) 1440 nm and (b) 1640 nm.

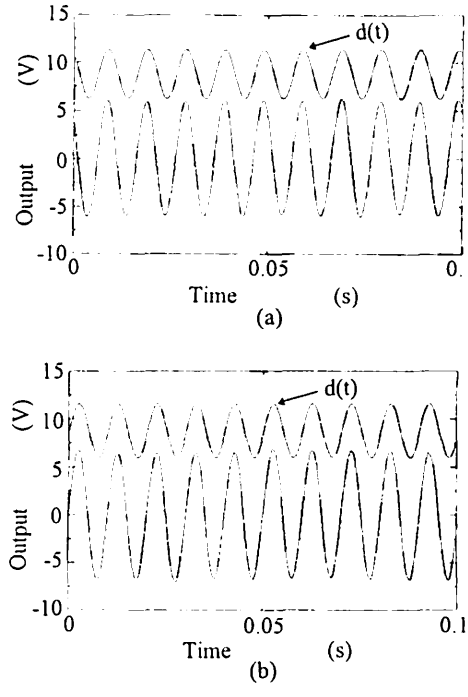

Fig. 6 Feedback signals observed when PI control was used. Lower traces are the feedback signals obtained when the amplitudes of $d(t)$ were (a) 1440 nm and (b) 1640 nm.

however, the observed signal no longer imitates the vibration of the mirror, as shown in Fig. 5(b). These measurements were carried out under the existence of an offset voltage, which was -3 V in this experiments. These correspond to the schematic explanation shown in Fig. 3(b). Thus the maximum measurable range was 1440 nm with this P control. If the offset voltage contained in the observed signal can be removed, the measurable range would be increased, as shown in Fig. 3(c).

The observed signal obtained when PI control was used are shown in Fig. 6. The P gain K_p and the integral I time T_I were 0.28 and 0.82 ms, respectively. When the amplitude of the vibration was 1440 nm, we obtained the signal shown in Fig. 6(a). The shapes of the measured signals shown in Figs. 5(a) and 6(a) were the same except for the offset voltage. Moreover, the observed signal was stable even if the amplitude became 1640 nm, as shown in Fig. 6(b), because the offset voltage was removed and the dynamic range became large.

Next, various vibration amplitudes were measured by using the P control and the PI control. Control parameters, the P gain K_p and the I time T_I, were as same as those in Figs. 5 and 6. Results are shown in Fig. 7, in which the measured voltages are converted to the vibration amplitude using Eq. (10). These agree quite well with a theoretical solid line. The measurement accuracy was 40 nm root mean square (rms) and there were no differences in the measurement accuracy in both control systems. The maximum measurable amplitude was 1440 nm with P control, but it was extended to 2000 nm with PI control. Therefore, the dynamic range with PI control was 1.4 times as large as that with P control. These results show that vibration measurement is possible if the feedback loop gain is known in advance, and that PI control is effective to extend the measurable range. It is considered that there are mainly two kinds of error sources. One of them is the phase change, which comes from the quite large external disturbance that was not eliminated by the feedback control. The other error source to be considered is the change of the amplitude of the feedback signal. This comes from the fluctuation of the optical axis and introduces the change of the gain K_f in the control system. It is not eliminated by the feedback control. Thus, to obtain high measurement accuracy, it is required to have high K_p and suppress the change of the visibility of interference signal.

Third, we investigated the influence of the P gain K_p and the I time T_I on the vibration measurements, respec-

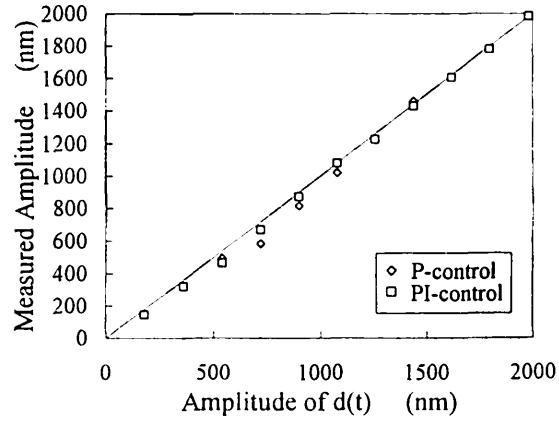

Fig. 7 Amplitudes of the sinusoidal vibration measured with the P control and the PI control.

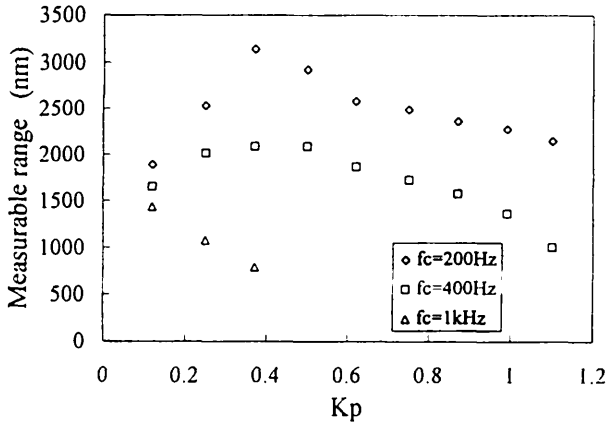

Fig. 8 Dependence of the measurable range on the proportional gain K_p.

tively. Figure 8 shows the dependence of the measurable range on K_p, where T_I was 0.82 ms. Although the response of the feedback loop becomes worse as the cutoff frequency of the LPF becomes small, the measurable range is extended. In this case, the LPF functions to stabilize the control system by reducing the frequency response. But large loop gain does not always contribute to measuring a large amplitude of vibration. Thus there is a suitable loop gain in the control system. The influence of the I time T_I on accuracy of vibration measurement is shown in Fig. 9. Various amplitudes of vibration whose vibration frequency was 100 Hz were measured by changing T_I. There are no differences in the measurement accuracy from 0.82 to 3.27 ms of T_I.

Finally, we measured triangular vibrations. The P gain K_p, I time T_I, and cutoff frequency of the LPF were 0.28, 0.82 ms, and 200 Hz, respectively. The measured result is shown in Fig. 10. The upper traces indicated by $d(t)$ are the driving signals applied to the PZT. The amplitude and frequency of the vibration were 1100 nm and 50 Hz, respectively. The observed signal imitated the vibration of the mirror very well. Furthermore, various amplitudes of the triangular vibration were measured by using the PI control. The measured result is shown in Fig. 11. It is confirmed that the triangular vibration can also be measured accurately, if the vibration frequency is small compared with the cutoff frequency of the LPF.

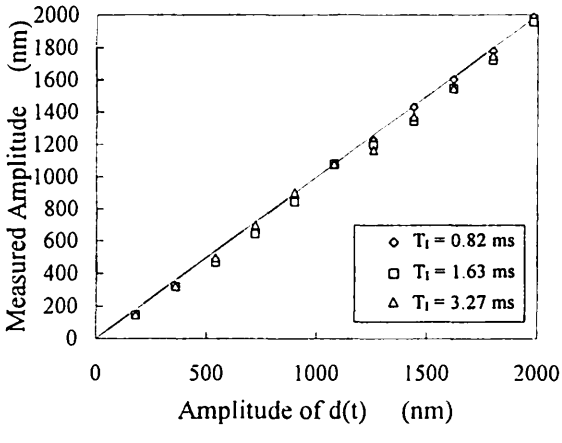

Fig. 9 Influence of the integral time T_I on accuracy of measurement of the sinusoidal vibration.

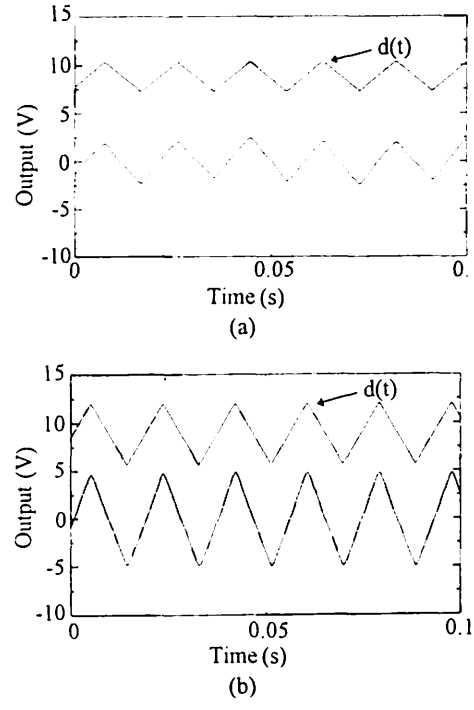

Fig. 10 Feedback signals observed when the PI control was used. Upper traces indicated by $d(t)$ are triangular driving signals applied to the PZT; lower traces are the feedback signals obtained when the amplitude of $d(t)$ were (a) 600 nm and (b) 1100 nm.

4 Conclusion

We have proposed a feedback type of interferometer with an optical fiber and clarified the characteristics of the system. Our mechanism has numerous advantages: (1) since it uses an optical fiber, the measurement probe can be placed at any desired location; (2) the simplicity of the optical system is maintained by virtue of the fact that it requires no

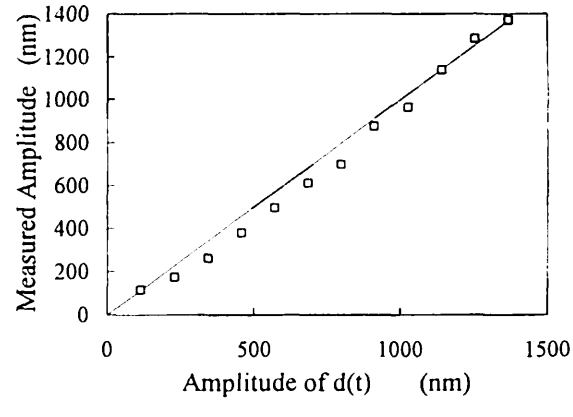

Fig. 11 Amplitudes of the triangular vibration measured with the PI control.

prepared reference mirror; (3) the wavelength tunability of the LD is used for direct phase modulation, thereby eliminating the need for a mechanical phase modulator; (4) measurements are carried out in real time, so phase unwrapping becomes unnecessary; and (5) the external disturbance is automatically removed. These experiments confirmed that a wide-range, disturbance-free, and real-time measurement is possible using this interferometer.

Acknowledgments

Part of this work was presented at the SPIE annual meeting[10] in Denver, Colorado. The authors are grateful to Dr. X. Wang for his useful suggestions and help in the experiments.

References

1. K. Tatsuno and Y. Tsunoda, "Diode laser direct modulation heterodyne interferometer," *Appl. Opt.* **26**, 37–40 (1987).
2. T. Yoshino, M. Nara, S. Mnatzakanian, B. S. Lee, and T. C. Strand, "Laser diode feedback interferometer for stabilization and displacement measurement," *Appl. Opt.* **26**, 892–897 (1987).
3. O. Sasaki, K. Takahashi, and T. Suzuki, "Sinusoidal phase modulating laser diode interferometer with a feedback control system to eliminate external disturbance," *Opt. Eng.* **29**(12), 1511–1515 (1990).
4. J. Liu, I. Yamaguchi, J. Kato, and T. Nakajima, "Active phase-shifting interferometer using current modulation of a laser diode," *Opt. Rev.* **3**(4), 287–292 (1996).
5. I. Yamaguchi, J. Liu, and J. Kato, "Active phase-shifting interferometers for shape and deformation measurements," *Opt. Eng.* **35**(10), 2930–2937 (1996).
6. T. Suzuki, O. Sasaki, and T. Maruyama, "Phase-locked laser diode interferometry for surface profile measurement," *Appl. Opt.* **28**(20), 4407–4410 (1989).
7. T. Suzuki, O. Sasaki, K. Higuchi, and T. Maruyama, "Phase locked laser diode interferometer: high speed feedback control system," *Appl. Opt.* **30**(25), 3622–3626 (1991).
8. T. Suzuki, O. Sasaki, K. Higuchi, and T. Maruyama, "Differential type of phase locked laser diode interferometer," *Appl. Opt.* **31**(34), 7242–7248 (1992).
9. O. Sasaki, K. Takahashi, "Sinusoidal phase modulating interferometer using optical fibers for displacement measurement," *Appl. Opt.* **27**(19), 4139–4142 (1988).
10. T. Suzuki, T. Okada, O. Sasaki, and T. Maruyama, "Feedback type of laser diode interferometer with an optical fiber," *Proc. SPIE* **2860**, 225–231 (1996).

Takamasa Suzuki received a BE degree in electrical engineering from the Niigata University in 1982, an ME-degree in electrical engineering from the Tohoku University in 1984, and a DrEng degree in electrical engineering from the Tokyo Institute of Technology in 1994. He is an associate professor of electrical and electronic engineering at the Niigata University. His research interests include optical metrology, optical information processing, and phase conjugate optics.

Takao Okada received his BE degree in electrical engineering from the Niigata University in 1996. He is currently pursuing his study toward an MS degree in electrical engineering at the Niigata University.

Osami Sasaki received BE and ME degrees in electrical engineering from the Niigata University in 1972 and 1974, respectively, and a DrEng degree in electrical engineering from the Tokyo Institute of Technology in 1981. He is a professor of electrical and electronic engineering at the Niigata University. His research interests include optical metrology, optical information processing, and phase conjugate optics.

Takeo Maruyama received a BE degree in electrical engineering from the Niigata University in 1965 and a DrEng degree in electrical engineering from the Nagoya University in 1979. He is a professor of electrical and electronic engineering at the Niigata University. His research interests include physics of ionized gases and optical metrology.